

Review

# Review on Boiling Heat Transfer Enhancement Techniques

Chandan Swaroop Meena <sup>1,2,\*</sup> , Ashwani Kumar <sup>3</sup> , Sanghati Roy <sup>4</sup>, Alessandro Cannavale <sup>5,\*</sup>   
and Aritra Ghosh <sup>6</sup> 

<sup>1</sup> CSIR-Central Building Research Institute, Roorkee 247667, India

<sup>2</sup> Academy of Scientific and Innovative Research (AcSIR), Ghaziabad 201002, India

<sup>3</sup> Technical Education Department Uttar Pradesh, Kanpur 208024, India

<sup>4</sup> Department of Mechanical Engineering, Birla Institute of Technology and Science, Pilani 333031, India

<sup>5</sup> Department of Civil Engineering Sciences and Architecture, Polytechnic University of Bari, 70126 Bari, Italy

<sup>6</sup> College of Engineering, Mathematics and Physical Sciences, Renewable Energy, University of Exeter, Penryn TR10 9FE, Cornwall, UK

\* Correspondence: chandanswaroop2008@gmail.com (C.S.M.); alessandro.cannavale@poliba.it (A.C.)

**Abstract:** Boiling is considered an important mode of heat transfer (HT) enhancement and has several industrial cooling applications. Boiling has the potential to minimize energy losses from HT devices, compared with other convection or conduction modes of HT enhancement. The purpose of this review article was to analyze, discuss, and compare existing research on boiling heat transfer enhancement techniques from the last few decades. We sought to understand the effect of nucleation sites on plain and curved surfaces and on HT enhancement, to suggest future guidelines for researchers to consider. This would help both research and industry communities to determine the best surface structure and surface manufacturing technique for a particular fluid. We discuss pool boiling HT enhancement, and present conclusions and recommendations for future research.

**Keywords:** heat transfer enhancement; boiling; nanofluids; droplets; pool boiling



**Citation:** Meena, C.S.; Kumar, A.; Roy, S.; Cannavale, A.; Ghosh, A.

Review on Boiling Heat Transfer Enhancement Techniques. *Energies* **2022**, *15*, 5759. <https://doi.org/10.3390/en15155759>

Academic Editors: Suvanjan Bhattacharyya, Kashif Ali Abro and Basma Souayah

Received: 27 May 2022

Accepted: 3 August 2022

Published: 8 August 2022

**Publisher's Note:** MDPI stays neutral with regard to jurisdictional claims in published maps and institutional affiliations.



**Copyright:** © 2022 by the authors. Licensee MDPI, Basel, Switzerland. This article is an open access article distributed under the terms and conditions of the Creative Commons Attribution (CC BY) license (<https://creativecommons.org/licenses/by/4.0/>).

## 1. Introduction

The concept of heat transfer refers to the flow of thermal energy through a process that involves a difference in temperature, subsequently leading to changes and redistribution of temperature. The study of transport phenomena involves the exchange of mass, momentum, and energy in the form of radiation, convection, and conduction. HT enhancement is a technique that can be utilized to improve the rate of heat removal. These techniques are further divided into two clusters: active and passive, as shown in Figure 1. Active enhancement techniques include ultrasonic enhancement and electrohydrodynamic, whereas the use of passive enhancement techniques can add extended surfaces, enhance thermal conductivity, and make surface or geometrical modifications to the flow channel by using inserts or additional devices, as shown in Figure 1. Here, our focus is to review passive techniques of heat transfer enhancement. The use of extended surfaces in industrial settings occupies a lot of space and leads to a larger thermal setup. Thus, thermal conductivity enhancements using boiling heat transfer is one of the most important known techniques for heat removal, unlike other conventional means. Boiling, unlike pure conduction, is a phase-changing process of convection and radiation that involves a high rate of heat transfer from a liquid to a vapour state. When a surface is exposed to liquid, and its saturation temperature exceeds that of the liquid, it becomes hot enough to cause boiling. This can be understood by the boiling curve, shown in Figure 2. Boiling has many industrial applications, such as in steam production, distillation, refining, dehydration, cooling of nuclear reactors, metallurgical processing, air conditioning, refrigeration and cryogenics, fluid handling and control, power systems, electronics cooling, on-orbit storage, microchip

cooling, chemical process industries, space systems, thermal management, food processing, health care processes, etc. The heat transfer rate/heat flux in boiling is calculated by using:

$$\dot{q} = \frac{\dot{Q}}{A} = h \cdot \Delta T_e \left[ \text{W} \cdot \text{m}^{-2} \right]$$

where  $h$  = HT Coefficient ( $\text{W}/(\text{m}^2 \cdot \text{K})$ ),  $A$  = Area ( $\text{m}^2$ ),  $\Delta T_e$  = Excess Temperature =  $T_{\text{surface}} - T_{\text{saturation}}$ ,  $T_s$  = Surface Temperature, and  $T_{\text{sat}}$  = Saturation Temperature of Liquid.

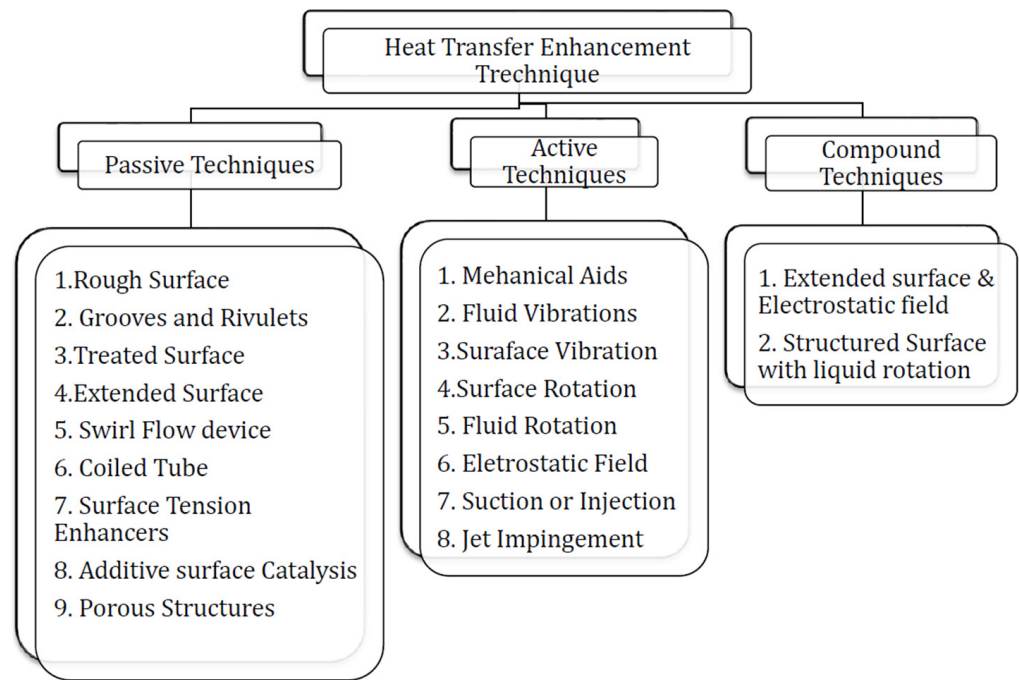


Figure 1. Heat transfer enhancement techniques.

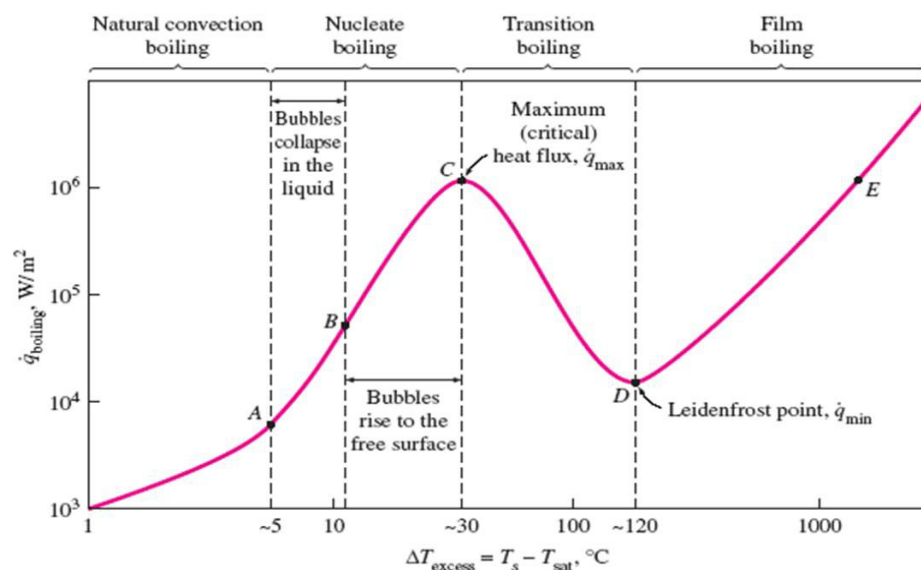


Figure 2. Boiling regimes, from Faghri & Zhang, 2006 [1].

Figure 2 represents all of the boiling regimes and the stages in which boiling phenomena occur. The first region shown in Figure 2 represents natural convection boiling, wherein liquid near the surface is slightly superheated. Near the surface of the liquid, boiling occurs in a thin layer. The superheated liquid moves up to the liquid–vapour interface, where

evaporation occurs. Fluid motion is determined primarily by the free convection effect. With increasing excess temperature, heat transfer increases.

In this review, HT enhancement techniques are described for smooth and curved surfaces, and we review background, enhancement techniques, and past research. Additionally, we outline our quantitative understanding of boiling heat transfer, citing various numerical conceptions on the subject, to qualitatively assess the current literature.

The second region in Figure 2 is the region on the curve from point A to C that represents nucleate boiling, wherein the liquid is overheated in relation to the saturation temperature, and vapor bubbles form at certain spots called active sites. These bubbles condense into liquid without reaching the liquid–vapor interface. Eventually, the bubbles grow in size due to increased pressure, temperature, and surface tension. On further increasing  $\Delta T_e$ , the bubbles start forming more rapidly and rise to the liquid surface, resulting in rapid evaporation. Due to bubble formation, agitation in the liquid occurs, leading to mixing and increases in heat flux and the boiling heat transfer coefficient.

The third region in Figure 2 represents transition boiling between partial nucleate boiling and unstable film boiling. Incoming fresh liquid is prevented from reaching the heating surface because of a bubble blanket. As bubbles form, a vapour film covers the surface (active sites). Due to a decrease in thermal conductivity, heat flux decreases, and  $K_{\text{liquid}} > K_{\text{vapour}}$ .

The fourth region in Figure 2 is the film boiling region where, with further increases in  $\Delta T_e$ , the vapour film is stabilized, active sites are covered by vapour blankets, and heat flux decreases to its lowest value. After that, radiation comes into play and there is a rapid increase in heat flux.

Our aim is to study nucleate boiling, where heat flux increases with increases in excess temperature, and to use other enhancement techniques, such as surface and geometrical modifications, for the same boiling regime in our experiment.

## 2. Surface Characteristics

Here, we shed light on some of the surface characteristics that has major effects on heat flux and on the heat transfer coefficient. Surface roughness and porosity are parameters that must be considered when enhancing the heat transfer rate. Both parameters are described below:

- Roughness was found to have a large effect on the heat transfer rate in one of the early research works by Jerome, 1960 [2]. With an increased roughness in a particular metal of particular geometry, there were greater occurrences of active nucleation sites. Having a higher density of sites may enhance the heat transfer coefficient.
- Porosity also enhances the heat transfer rate. Surface porosity can be increased by manually/artificially creating cavities on the surface.

Utilizing the above-mentioned surface modifications and a cylindrical surface as the geometric modification, this experiment aimed to increase the rate of heat transfer, and investigate how these passive heat transfer enhancement techniques affected the heat transfer rate. We also compared the heat transfer rate through a flat surface versus a cylindrical surface by plotting a  $q$  versus  $\Delta T_e$  graph.

## 3. Background of Boiling Heat Transfer

Nukiyama, 1934 [3] ran the very first study on boiling heat transfer in Japan. He experimented with saturated pool boiling around an electrically heated platinum wire. The boiling regimes shown in Figure 2 was partially discovered by Nukiyama. He plotted nucleate boiling and film boiling on a  $q$ .  $T$  plot but was unable to explain the process between nucleate and film boiling, which is now known as transition boiling. The studies of Nukiyama were later validated by Drew and Mueller, 1937 [4] through experiments performed on an organic liquid. Since then, there have been numerous studies performed on various subtopics related to nucleate and film boiling, and boiling heat transfer.

Guo et al., 1998 [5] proposed a new approach to the convective heat transfer energy equation. They noted that enhancement of the synergetic effect between velocity and temperature could be increased by raising mean heat convection intensity and the dimensionless temperature difference. This could be achieved using a combination of methods. According to the field synergy principle, increasing the synergy between the velocity and heat flow fields may result in an increase of heat transfer. This is useful in various engineering fields as it can reduce flow resistance and improve the efficiency of a system. The synergistic interaction between the velocity vector and the temperature gradient is quantified by the field synergy angle. Thus, heat transfer augmentation could be accomplished using this approach. Then, the authors introduced heat convection velocity. The first step in this process was to explore the mechanism by which heat convection velocity could be generated in a smooth circular tube. The heat transfer in the circular tube was then improved by creating a new insert. An analysis of heat convection velocity was carried out to study various aspects of the enhanced tube.

#### 4. Techniques to Improve Heat Exchange

Heat transfer enhancement is the process of increasing the heat transfer rate (or improving performance, to be more precise). There have been numerous studies on the methods of enhancing heat transfer.

Bergles, 1997 [6] categorized both active and passive techniques used in improving heat transmission. Figure 1 illustrates the classification of heat transfer enhancement techniques, with examples. Calmidi and Mahajan, 2000 [7] performed an experimental and numerical study on aluminum metal foams with high porosity for single-phase forced convection. They found good agreement between the numerical results and their experimental findings. Mori and Okuyama, 2009 [8] investigated pool boiling using a honeycomb porous media. The critical heat flux (CHF) increased approximately 2.5 times more than on a plain surface. They also calculated CHF performance with capillary suction, permeability, pore radius, wall thickness, height of the porous media, and vapour scope channels.

Cooke et al., 2010 [9] calculated the bubble dynamics and heat transfer performance on microchanneled copper surfaces. They concluded that an increase in heat flow affected the average bubble diameter, porosity, and pore diameter, as well as the contact angle, distance from the channel bottom, and porosity. However, having high porosity and a large average particle diameter resulted in a local thermal effect with no equilibrium between the working fluid and the surface heating area; heat transfer enhancement diminished at high and moderate mass fluxes. Due to the high fluxes, the liquid did not replace the vapour, resulting in increased vapour blankets and drying out. Liter and Kaviany, 2001 [10] also researched CHF enhancement. They used a modulated porous layer for pool boiling. The liquid and vapor flow routes were found to be directly related to the heat transfer porous coating structure. The deep porous-layer coating had the worst performance whereas the artery evaporator system with fully segregated liquid and vapour flow channels had good performance. Recently, Meena and Das, 2022 [11] ran an experiment with a large diameter cylinder, and reported bubble sliding and merging phenomena.

Hao et al., 2017 [12] studied the effects of using deformable structures in pool boiling on CHF. They used ethanol, FC-72, and water as working fluids, and significantly reduced the superheat wall temperature at the same heat flux. Wang et al., 2020 [13] used a porous honeycomb plate under sub-cooled flow boiling to increase the critical heat flux. They successfully found an improvement ratio of around 2.4 times using porous media, compared with a plain surface, using water as the working fluid. In sub-cooled flow boiling, the mass flux, system pressure, intake sub-cooling, and bubble behavior all have a direct impact on the heat flux.

Koncar et al., 2013 [14] concluded the design and secure operation of nuclear reactor systems based on studies of heat transfer and phase change in two-phase flow. The complex processes found in nuclear reactor systems, particularly during transient operation, need considerable theoretical and experimental study. The findings of this paper verified the

potential for 3D simulation of sub-cooled flow boiling in industrial applications. Several model enhancements were also recommended to produce more accurate predictions. Siddique et al., 2010 [15] described and reviewed the following heat transfer enhancers: protrusions, porous media, big particle suspensions, nanofluids, phase-change devices, flexible seals, flexible complex seals, extended surfaces, vortex generators, and composite materials with extremely high thermal conductivity. Methods described in the literature include the use of joint-fins, fin roots, fin networks, bi-convections, permeable fins, porous fins, helical micro fins, and complicated twisted tape designs. We determined that single-phase heat transfer enhanced with micro fins should be used more to decrease discrepancies between studies. More research needs to be done to elucidate how a nanofluid enhances heat transfer primarily through these mechanisms. Furthermore, researchers should pay close attention to the order in which they calculate the degrees to which flexible/flexible-complex seals promote heat transfer, flow, and heat transfer inside a convective medium. This summarizes the active mechanical enhancing methods that enhance heat transfer.

Khaled and Vafai, 2014 [16] introduced flexible fluidic thin films in their work. They provided details of a novel passive technique to improve the cooling capacity of fluidic thin films. Additionally, they claimed that when there is a greater pressure drop in the flexible microchannel, the average velocity increases, expanding the microchannel and resulting in an increase in cooling capacity (increased flow rate of coolant). Sandeep and Malvandi, 2016 [17] in their review paper, observed that nanoparticles should not pose any major issues (abrasion, clogging, fouling, or increased pressure loss in heat exchangers) compared with larger particles because they have higher thermal conductivity than the working fluid and are similar in size to the molecules of the base fluid. As nanoparticles increase the thermal conductivity of common cooling fluids, including water, oil, and ethylene-glycol, they aid in the development of more effective heat exchange equipment. A theoretical inquiry was then conducted on how nanoparticle migration affects the improvement of heat transmission during film boiling of nanofluids across a vertical cylinder. Different types of nanoparticles were considered, namely titania and alumina. Due to thermophoresis, nanoparticles not uniformly distributed in the film were able to accumulate at the heated wall. This led to enhanced heat transfer rates. Nevertheless, there was a trade-off between thermal conductivity reduction and an increase in temperature gradient at the wall, which determines the net enhancement/deterioration of the heat transfer rate.

Al-Zaidi et al., 2019 [18], investigated the impact of the channel aspect ratio on HFE-7100 flow boiling properties, including flow patterns, heat transmission, and pressure drop in copper multi-microchannel heat sinks. The average surface roughness of the channel bottom surface was nearly the same in the three heat sinks, with a base area of 500 mm<sup>2</sup> and channel hydraulic diameter of 0.46 mm. The HFE-7100 flow boiling experiments were carried out in horizontal multi-microchannel heat sinks. The flow patterns that were observed included bubbly, slug, churn, and annular flow. There were also small nucleating bubbles visible in the annular flow liquid film. Forward motion, stagnation period, and backward motion were discovered to represent the flow reversal cycle. As a result of this flow reversal, pressure drop fluctuated more in channels with small aspect ratios. The heat transfer coefficient was larger when vapor quality was low, but decreased as vapour quality rose. The amount of heat that could be removed from the chipset (base heat flow) increased with a reduced channel aspect ratio. Further study of other aspect ratio ranges, operational conditions, and working fluids is required to validate these findings. Table 1 shows a comparison of the existing literature on heat transfer enhancement.

**Table 1.** Comparative study of different approaches of heat transfer enhancement.

Author	Working Fluid	Parameters	CHF Enhancement
You et al., 2003 [19]	Al <sub>2</sub> O <sub>3</sub> /water (nanofluid)	0–0.05 g/L, test heater: Cu	200%
Coursey et al., 2008 [20]	Al <sub>2</sub> O <sub>3</sub> /ethanol (nanofluid)	0.001–10 g/L, test heater: Glass	25% (at 10 g/L)
El-Genk et al., 2008 [21]	FC-72	Porous graphite surface	41%
Satyamurthi et al., 2009 [22]	PF-5060	MWCNTs (nanomaterial), boiling surface material: Si	58%
Park et al., 2010 [23]	Graphene (nanofluid)	0.001% by vol., test heater: Ni-Cr wire	84%
Sheikhbahai et al., 2012 [24]	Fe <sub>3</sub> O <sub>4</sub> /water/Ethylene glycol (nanofluid)	0.01–0.1% by vol., test heater: Ni-Cr wire	100% (at 0.1% conc.)
Tang et al., 2012 [25]	Water	Cu-Zn alloy nanoporous surface, 50–200 nm pore size	enhanced
Betz et al., 2013 [26]	DI water	SiO <sub>2</sub> (50 nm coating thickness) (nanomaterial), surface modification technique: SBPi (SHPi and SHPo), test surface: Si	300%
Dai et al., 2013 [27]	–	CNT (nanomaterial), surface modification technique: HPo-HPi MWCNT composite, test surface: Cu	16%
Han kim et al., 2015 [28]	R-123, DI water	Al (nanomaterial), boiling surface material: Cu	40% (8–12 μm size and R-123)
Bostanci et al., 2015 [29]	HFE-7100	TiO <sub>2</sub> (nanomaterial), surface modification technique: HPo/HPi (pattern size 40, 100, 250 μm), test surface: Cu	47%
Jun et al., 2016 [30]	DI water	Cu (nanomaterial), boiling surface material: Cu	2 times (enhanced with coating thickness)
Gao et al., 2016 [31]	Water	Nanoporous Cu surface, 50–200 nm pore size	enhanced
Hu et al., 2017 [32]	Water	Nanoporous Al alloy surface	112%
Kumar et al., 2017 [33]	FC-72	CuNW (nanomaterial), particle size: 35–200 nm, boiling surface material: Cu	48%
Seo et al., 2017 [34]	DI water	MWCNTs/polyethy leneimine (nanomaterial), boiling surface material: SS	94%
Gu et al., 2018 [35]	Ag-CNT/water (nanofluid)	0.1%, 0.3%, 1% mol.	21%

## 5. Heat Transfer Enhancement in Heat Exchangers

There have been numerous studies in the field of heat exchangers on how to improve the ability to transfer heat by using different types of inserts and tube geometries.

Abdel-Rahmen et al., 1996 [36] demonstrated that the perfect tape width exists, and to see the best thermohydraulic performance, researchers need to pay attention to the Reynolds number and twist ratio. Freund et al., 2004 [37] also studied hydraulic and

thermal performance when tape was inserted in a large, hydraulic diameter annulus in the shape of a twist. This research has led to other similar research. Promvonge et al., 2007 [38] studied circular tubes with twisted tapes and saw that the heat transferability of a conventional heat exchanger increases when twisted tapes are introduced. Nanan et al., 2014 [39] examined the effect on heat transfer when helical screw tape was used, in a double pipe, both with and without a core rod; they concluded that helical screw tape used without the core rod gave better results than with the core rod. Thianpong et al., 2012 [40] tested the heat transfer coefficient and friction factor values for various twisted and wing cut ratio values.

Thianpong et al., 2012 [41] also studied twisted cassettes with alternating counter-clockwise and clockwise directions, from which clockwise twisted tapes were found to be better at heat transfer. Wongcharee et al., 2011 [42] compared twisted tapes with alternating wings along the axis as inserts and found that alternating wings were better at heat transfer. Another study by Eiamsa-Ard et al., 2010 [43] found that temperature-transfer efficiency and the friction factor value was maximized when the twist ratio for alternate twisted tapes in clockwise and counterclockwise directions was set to three. Eiamsa-Ard et al., 2010 [44] further validated that a tube with a twist ratio of three is better at heat transfer. Eiamsa-Ard et al., 2009 [45] observed the greatest rate of heat transmission in the tube when it was connected with a conical ring and twisted tape, compared with smooth tubes.

Thianpong et al., 2012 [41] experimented with twisted tapes and ring turbulators in a circle with varying ratios of pitch and twist. A combination of a circular ring and tapes showed maximum thermal performance compared with a pitch ratio and twist ratio of one and three, respectively. Eiamsa-Ard et al., 2009 [45] studied consistent and irregular twisted tapes with alternative axes for Reynolds numbers ranging from 5K to 21.5K. They concluded that a tube using twisted tapes with alternate axes that are non-uniform and has the smallest value of alternate length to twist length ratio is better at heat transfer. Eiamsa-Ard et al., 2010 [43] also studied the effects of serrated-edge twisted tapes on the performance of heat exchangers and concluded that increasing the width ratio and decreasing the depth ratio enhances performance.

Promvonge et al., 2012 [46] found that a dimpled tube with inserted twisted tape had a high friction factor, more convective heat transfer, and overall, more efficient convective heat transfer than a smooth dimpled tube. Skullong et al., 2016 [47] used twisted tape with perforations and parallel wings to improve heat transfer in a circular tube. Wings produced obstacles and perforations reduced the friction factor by releasing the flow. They concluded that thermal performance is maximized when the hole diameter ratio is minimized and wing depth ratio is maximized. Pethkoolet al., 2010 [48] compared helically corrugated tubes and smooth tubes and concluded that helically corrugated tubes are better at heat transfer and have higher values of the heat transfer coefficient when compared with a smooth tube. Nanan et al., 2014 [39] studied perforated helical twisted-tape inserts, keeping the twist ratio constant and varying the ratios between the diameter and perforation pitches. They found that when the perforation diameter decreases and perforation pitch increases, thermal performance factor also increases. Using twisted tape with perforation decreased the intensity of turbulence and area of blockage, resulting in reduced friction and a reduced heat transfer rate, unlike when inserted with a solid insert.

Kongkaietpaiboon et al., 2010 [49] also studied solid and perforated conical rings and found that reducing the pitch ratio and number of perforated holes increased the heat transfer rate and friction factor of perforated conical rings; however, the thermal performance factor rose when the pitch ratio and number of perforated holes were reduced. Guo et al., 2011 [50] tested center-cleared twisted tape used as inserts in a circular tube, and found improved thermohydraulic performance. By cutting the edges of twisted tapes to a narrow width, thermohydraulic performance was degraded. Chang et al., 2007 [51] compared tapes with a different number of twists, ranging from one to three, and concluded that triple twisted tapes showed the highest performance factors for turbulence. Kathait and Patil, 2014 [52] studied the heat transfer and frictional losses in a heat exchanger tube

as a function of discrete corrugated rib roughness and found that a corrugated tube with five gaps improved the Nusselt number and friction factor.

Vashistha et al., 2016 [53] reported in a review that studies using twisted tapes with a twist ratio of 2.5 significantly increased heat transfer, with a comparable increase in friction losses, compared with a smooth tube. The highest heat transfer rate and friction enhancements were determined to be 2.42 and 6.96 times that of a smooth tube, respectively. Li et al., 1982, [54] using high speed and flow visualization, explained the flow structure of helically finned tubes. They employed one to three fin beginnings, four tubes with rounded ribs, and helix angles between 38 and 80° in their investigation. It was observed from photographs that there were parabolic patterns of bubbles in laminar flow. These patterns break in turbulent flow, due to random separation vortices. Li et al., 1982 [54] found that both spiral pattern and boundary-layer separation flow occurred in helical ridging tubes; however, they occurred with different intensities in the tubes, having different configurations. Wen et al., 2004 [55] showed that maximum enhancement occurs at an axial distance of approximately a hundred times more than the tube diameter.

## 6. Nanofluids

In recent years, energy consumption has exponentially increased for things such as electronic devices, nuclear power reactors, the cooling of rocket nozzles, etc. Thermal management is classified into single-phase and two-phase heat transfer. Two-phase heat transfer has higher heat transfer efficiency compared with single-phase heat transfer; however, this process is very complicated, and involves bubble formation, condensation, vapour quality, flow boiling geometry, liquid subcooling temperature, etc. Therefore, new technologies such as making surface modifications, decreasing flow area dimensions, using nanofluids and porous media structures, etc., have been proposed by researchers to increase the heat flux and CHF. In a variety of heat transfer applications, including heat exchangers, cooling of electronic equipment, and chemical processes, nanofluids are considered the heat transfer fluid of the future. Small solid particles suspended in energy transmission fluids can increase thermal conductivity, which is an efficient and creative technique to greatly improve heat transfer properties. Numerous researchers have run experimental and numerical studies to investigate the use of nanofluids to manage heat transfer, due to their expanding use in applications in recent years. Nanofluids have been shown to improve critical heat flux under pool boiling conditions due to deposits of the nanoparticle on the heater surface (Kim et al., 2007 [56]). The use of nanofluid in buildings was investigated by Amirahmad et al., 2021 [57].

Gunnasegaran et al., 2012 [58] studied numerical simulations of nanofluid flow. They discussed two types of compact heat exchangers (CHE): thermal and hydraulic. Thermal and hydraulic CHEs were studied using conventional coolant to determine how nanofluids affect factors such as heat transfer coefficient variation, shear stress skin friction, pressure drop, and pumping power as a function of the Reynolds number. Maddah et al., 2014 [59] studied heat transfer in a double-pipe heat exchanger fitted with twisted-tape elements and titanium dioxide nanofluid.

Maddah et al., 2018 [60] explored the increase in heat transfer in a twin-pipe heat exchanger using a nanofluid combining water and aluminium oxide nanoparticles in turbulent flow. The heat transfer values were determined in the nanofluid turbulent flow, containing 20 nm aluminium oxide suspended particles in water at a volume concentration of 0.1–0.3%. According to a comparison based on a fixed Reynolds number, the heat transfer coefficient and Nusselt number of the nanofluid increased by 15 to 20% compared with the base fluid. The addition of nanoparticles to the fluid increased the average heat transfer coefficient in the turbulent flow regime. The Reynolds number increased together with the overall heat transfer coefficient. Two potential causes of this increase were the use of a nanofluid with suspended nanoparticles that could have enhanced the thermal conductivity of the mixture, or a high energy exchange process that was brought on by the amorphous mobility of the nanoparticles.



Sandeep et al., 2016 [17], in their review paper, observed that nanoparticles pose less of a risk for heat exchanger problems, such as abrasion, clogging, fouling, and additional pressure loss, than bigger particles. This is due to their similar size to the molecules of the base fluids and higher thermal conductivity than the working fluids. The inclusion of nanoparticles helps in the construction of more efficient heat exchange equipment, as they improve thermal conductivity of regular cooling fluids, such as water, oil, and ethylene-glycol. A theoretical inquiry investigated how nanoparticle migration affects the improvement of heat transmission during film boiling of nanofluids across a vertical cylinder. Two different kinds of nanoparticles, titania and alumina, were taken into consideration. Their effectiveness in accelerating the rate of heat transfer was investigated. Nanoparticles that are not evenly dispersed throughout the film can gather at the heated wall due to thermophoresis. This results in increased heat transmission rates. The net improvement or decrement in the heat transfer rate, however, depends on the trade-off between a decrease in thermal conductivity and an increase in the temperature gradient at the wall. In order to improve this performance, Freitas et al., 2021 [61] investigated combining personalised surface modifications with the usage of nanofluids.

## 7. Effect of Droplet Dynamics on Heat Transfer

During droplet spreading and receding phases below the saturation temperature, droplet temperature changes spatially and temporally, making it difficult to measure.

Pasandideh-Fard et al., 2002 [62] studied the effect of droplet diameter on heat transfer characteristics when a droplet falls onto a flat or smooth surface, and developed a mathematical model for this process. Larsen et al., 2011 [63] conducted numerical simulations and presented a modified equation of cooling effectiveness for smooth surfaces. Roisman, 2009 [64] with the help of the N-S equation and energy transport equation, examined the flow and heat transfer characteristics of impinging droplets with consideration of phase change. Herbert et al., 2013, [65] with the help of dimensionless numbers, also studied heat transfer during droplet impact. Another study by Ahn et al., 2012 [66] looked at the behavior of an impinging droplet on a heated textured surface, and examined the variation in the evaporating meniscus by measuring the dynamic contact angle. There have been several other studies by Alizadeh et al., 2012, Negeed et al., 2014, Tran et al., 2012 [67–69] on spreading and receding dynamics, the effect of surface smoothness, phase change of droplet impacts on heated rough surfaces, and the Leidenfrost phenomena of a droplet on a textured surface; however, there is a deficiency of experimental data.

A study by Moon et al., 2016 [70] suggested a modified equation for total thermal energy and studied the cooling effectiveness for the three types of wetting surfaces, i.e., partial, non-wetting, and total wetting. Due to the holes of the textured surface, a liquid droplet spreads and penetrates the surface, leading to the formation of the air pockets. When this phenomenon occurred on a heated surface, it resulted in the recoil of diameter, although initially the contact diameter increased. This was because the viscosity of the thin layer of liquid decreased on the heated surface.

### 7.1. Nucleate Boiling over Plane Surface

Zuber, 1958 [71] described methods to determine CHF based on hydrodynamic instability. Mikic and Rohsenow, 1969 [72] gave a model for flat surfaces. The micro-conduction in their model occurred at the nucleation site and everywhere else took place by natural convection. Bhat et al., 1983 analyzed the effect on heat transfer enhancement using the macrolayer. Later in 1986, they also reported the experimental values of the initial macrolayer thickness and frequency of vapour mass for water. Prasad et al., 1985 [73] also developed a HT model using similar assumptions as Bhat et al., 1983 [74]. Jairapuri and Saini, 1991 [75] developed a HT model assuming constant wall heat flux into the macrolayer; it predicted average conduction heat flow rates at the liquid–vapour interface that were in excellent agreement with the experimental values of input heat flux. Among the other efforts on the near-field model, Pasamehmetoglu et al., 1993 [76] described the dry out of

microlayer and macrolayer. Brief reviews of these models have been presented by Katto, 1994 and Lienhard, 1994 [77,78]. Das and Roetzel, 2008 [79] developed a composite heat transfer model for pool boiling on horizontal tubes. Their model shows good agreement with experimental results reported in their paper and reported in the literature. Sateesh et al., 2005 [80] developed a model to predict heat transfer phenomena over an inclined surface as well as in a horizontal cylinder. Qu et al., 2017 [81] used the Eulerian two-fluid model to observe formation and detachment of a bubble at the nozzle mouth.

### 7.2. Nucleate Boiling over Cylindrical Surface

Due to the many applications of tubes in industries, research on curved surfaces has also increased. Bubbles can form around a cylindrical surface having a smaller diameter than the bubble departure diameter. On the other hand, boiling becomes important over finite-sized cylinders, in the case of nuclear rod bundles. Ribatski and Jabardo, 2003 [82] ran an experimental investigation on the saturated pool boiling of halocarbon refrigerants on cylindrical surfaces made of different materials. Elghanam et al., 2011 [83] studied the effect of surfactants on boiling. Their results showed that surfactants significantly increased the heat transfer rate. The effect of the angle of inclination in a straight rounded-base tunnel was given by Das et al., 2009 [84]. Mehta and Kandlikar, 2013 [85] conducted experiments on pool boiling heat transfer over enhanced cylindrical micro-channel test surfaces with water, at atmospheric pressure. Meena et al. 2017 [86] studied neighboring nucleation site interactions. Deep et al. 2017 [87] studied boiling over spherical surfaces.

## 8. Numerical Conceptions in Boiling Heat Transfer

Yamagata et al., 1955 [88] proposed the following relationship and fit the existing experimental data as:

$$q \propto T_{sat}$$

Subsequently, many researchers have developed correlations, but all of these correlations face limitations, as these are only valid for certain operating conditions.

Kurihari and Meyers, 1960 [89] boiled water and various organic liquid on a roughened copper surface and obtained satisfactory results. They have also related the heat transfer coefficient,  $h$ , with the number of nucleation sites per unit area,  $n_s$ , as:

$$h \propto n_s^{0.43}$$

Hsu and Schmidt, 1961 [90] first proposed the idea that a vapour embryo would grow into a bubble if the liquid temperature of the embryo tip was equal or higher than the saturation temperature of the pressure corresponding to the bubble. The functional dependence of superheat and size of the cavity that will nucleate first was obtained by Hsu and Schmidt (1961) [90] as:

$$D_c = \sqrt{\frac{8f_1(\varphi)2T_s\delta\sigma}{f_2(\varphi)h_{fg}\rho_g\Delta T_{sat}}}$$

Here,  $\delta$  is the thickness of the equivalent thermal layer and  $f_1(\varphi)$  depends on the contact angle  $\varphi$ . Later, Hsu, 1962 [91] substantiated that for favorable blossoming of the bubble embryo, the top liquid layer should be warm. The bubble embryo will shrink if the required superheat does not exist. By incorporating concepts related to the thermal boundary layer,  $\delta_t$ , he proposed the following criterion for incipient superheat:

$$\Delta T_t = \frac{8f_2(\varphi)\sigma T_{sat}}{\rho v h_{fg} \delta_t}$$

After gaining knowledge about individual bubble evolution, researchers tried to understand the dependence of activation site density on heat transfer enhancement.

According to Hsu and Graham, 1976 [92], the density of active nucleation sites increases approximately as the square of the heat flux. From their earlier experimental

observations, Gaertner and Westwater, 1960 [93] obtained the number density of active nucleation sites ( $N_a$ ) as:

$$N_a \propto q^{2.1}$$

On the other hand, Cornwell and Brown, 1978 [94] found dependence of  $N_a$  on wall superheat as:

$$N_a = \Delta T_w^{4.5}$$

Functional temporal dependence of the bubble radius has been established by Rohsenow et al., 1952 [95] as:

$$r(t) = \left[ \sqrt{\left[ \frac{2(T_f - T_{sat})P_f}{3T_{sat}P_f} \right] \left[ \frac{h_{fg}\rho_g}{P_f} \right]} \right] t$$

Here,  $r(t)$  is the time-dependent bubble radius,  $T_f$  is the liquid temperature,  $[T_{sat} (P_f)]$  is the saturation temperature at the corresponding liquid pressure,  $h_{fg}$  is the latent heat of vapourization,  $t$  is time, and  $\rho_g$  and  $\rho_f$  are the vapour and liquid densities, respectively.

## 9. Conclusions/Analysis of Existing Work and Future Possibilities

There have been various studies on the use of passive techniques for structured surfaces to increase rates of heat transfer. There have also been experiments on both continuous and discrete nucleation sites; however, further investigation is needed to understand the interaction between nucleation sites. In most cases, the structured surfaces have been flat, and very rarely cylindrical; thus, there is a limitation of studies on boiling over a cylindrical surface. For cylinders with a smaller diameter than the radius of departure, and large-sized cylinders, there is a need for more studies on the formation, growth, and departure of bubbles.

**Author Contributions:** Conceptualization, C.S.M.; methodology, C.S.M., A.K., A.C. and A.G.; validation, A.K., S.R. and A.G.; formal analysis, C.S.M., A.K., A.C. and A.G.; investigation, C.S.M., A.G. and A.C.; writing—original draft preparation, C.S.M.; writing—review and editing, C.S.M., A.G., A.K., S.R. and A.C.; visualization, C.S.M., A.C. and A.G.; supervision, C.S.M.; project administration, C.S.M.; funding acquisition, C.S.M., A.G. and A.C. All authors have read and agreed to the published version of the manuscript.

**Funding:** This research received no external funding.

**Acknowledgments:** The study presented forms a part of the research carried out at CSIR—Central Building Research Institute and is published with the permission of the Director.

**Conflicts of Interest:** The authors declare no conflict of interest.

## Nomenclature

$A$	Area of copper cylinder, $m^2$
$CHF$	Critical heat flux, $W/m^2$
$f$	Frequency of variations
$h$	Convective heat transfer coefficient, $W/m^2 K$
$h_{fg}$	Latent heat of vapourization, $J/kg$
$K$	Thermal Conductivity, $W/m K$
$n_s$	Number of nucleation sites per unit area
$p_f$	Liquid pressure, $N/m^2$
$Q$	Rate of heat transfer, $W$
$q$	Heat Flux, $W/m^2$
$T_f$	Liquid Temperature, $^{\circ}C$
$T_{sat}$	Saturation temperature of liquid, $^{\circ}C$

$t$	Time, sec
$V$	Voltage, V
Greek Symbols	
$\Delta T$	Superheat, K
$\rho_g, \rho_f$	Vapor and Liquid densities respectively, kg/m <sup>3</sup>
$\sigma$	Surface tension of liquid vapour interface, N/m

## References

- Faghri, A.; Zhang, Y. *Transport Phenomena in Multiphase Systems*; Academic Press: Cambridge, MA, USA, 2006; pp. 765–852.
- Jerome, B.P. *Transition Boiling Heat Transfer from a Horizontal Surface*; Massachusetts Institute of Technology, Division of Industrial Cooperation: Cambridge, MA, USA, 1960.
- Nukiyama, S. The maximum and minimum values of the heat transmitted from metal to boiling water under atmospheric pressure. *Jpn. Soc. Mech. Eng.* **1934**, *37*, 367–378.
- Drew, T.B.; Mueller, A.C. Boiling. *Trans. AIChE* **1937**, *33*, 449–473.
- Guo, Z.Y.; Li, D.Y.; Wang, B.X. A novel concept for convective heat transfer enhancement. *Int. J. Heat Mass Transf.* **1998**, *41*, 2221–2225. [[CrossRef](#)]
- Bergles, A.E. Enhancement of pool boiling. *Int. J. Refrig.* **1997**, *20*, 545–551. [[CrossRef](#)]
- Calmidi, V.V.; Mahajan, R.L. Forced Convection in High Porosity Metal Foams. *J. Heat Transf.* **2000**, *122*, 557–565. [[CrossRef](#)]
- Mori, S.; Okuyama, K. Enhancement of the critical heat flux in saturated pool boiling using honeycomb porous media. *Int. J. Multiph. Flow* **2009**, *35*, 946–951. [[CrossRef](#)]
- Cooke, D.; Kandlikar, S.G. Pool boiling heat transfer and bubble dynamics over plain and enhanced microchannels. In Proceedings of the International Conference on Nanochannels, Microchannels, and Minichannels, Montreal, Quebec, Canada, 1–5 August 2010; Volume 54501, pp. 163–172.
- Liter, S.G.; Kaviani, M. Pool-boiling CHF enhancement by modulated porous-layer coating: Theory and experiment. *Int. J. Heat Mass Transf.* **2001**, *44*, 4287–4311. [[CrossRef](#)]
- Meena, C.S.; Das, A.K. Boiling Heat Transfer on Cylindrical Surface: An Experimental Study. *Heat Transf. Eng.* **2022**, 1–13. [[CrossRef](#)]
- Hao, W.; Wang, T.; Jiang, Y.-Y.; Guo, C.; Guo, C.-H. Pool boiling heat transfer on deformable structures made of shape-memory-alloys. *Int. J. Heat Mass Transf.* **2017**, *112*, 236–247. [[CrossRef](#)]
- Wang, K.; Gong, H.; Wang, L.; Erkan, N.; Okamoto, K. Effects of a porous honeycomb structure on critical heat flux in downward-facing saturated pool boiling. *Appl. Therm. Eng.* **2020**, *170*, 115036. [[CrossRef](#)]
- Koncar, B.; Krepper, E.; Bestion, D.; Song, C.-H.; Hassan, Y.A. Two-Phase Flow Heat Transfer in Nuclear Reactor Systems. *Sci. Technol. Nucl. Install.* **2013**, *2013*, 1–2. [[CrossRef](#)]
- Siddique, M.; Khaled, A.R.; Abdulhafiz, N.I.; Boukhary, A.Y. Recent Advances in Heat Transfer Enhancements: A Review Report. *Int. J. Chem. Eng.* **2010**, *2010*, 106461. [[CrossRef](#)]
- Khaled, A.-R.; Vafai, K. Heat transfer enhancement by layering of two immiscible co-flows. *Int. J. Heat Mass Transf.* **2014**, *68*, 299–309. [[CrossRef](#)]
- Sandeep, N.; Malvandi, A. Enhanced heat transfer in liquid thin film flow of non-Newtonian nanofluids embedded with graphene nanoparticles. *Adv. Powder Technol.* **2016**, *27*, 2448–2456. [[CrossRef](#)]
- Al-Zaidi, A.H.; Mahmoud, M.M.; Karayiannis, T.G. Flow boiling of HFE-7100 in microchannels: Experimental study and comparison with correlations. *Int. J. Heat Mass Transf.* **2019**, *140*, 100–128. [[CrossRef](#)]
- You, S.M.; Kim, J.H.; Kim, K.H. Effect of nanoparticles on critical heat flux of water in pool boiling heat transfer. *Appl. Phys. Lett.* **2003**, *83*, 3374–3376. [[CrossRef](#)]
- Coursey, J.S.; Kim, J. Nanofluid boiling: The effect of surface wettability. *Int. J. Heat Fluid Flow* **2008**, *29*, 1577–1585. [[CrossRef](#)]
- El-Genk, M.S.; Parker, J.L. Nucleate boiling of FC-72 and HFE-7100 on porous graphite at different orientations and liquid subcooling. *Energy Convers. Manag.* **2008**, *49*, 733–750. [[CrossRef](#)]
- Sathyamurthi, V.; Ahn, H.-S.; Banerjee, D.; Lau, S.C. Subcooled Pool Boiling Experiments on Horizontal Heaters Coated With Carbon Nanotubes. *J. Heat Transf.* **2009**, *131*, 071501. [[CrossRef](#)]
- Park, S.D.; Lee, S.W.; Kang, S.; Bang, I.C.; Kim, J.H.; Shin, H.S.; Lee, D.W. Effects of nanofluids containing graphene/graphene-oxide nanosheets on critical heat flux. *Appl. Phys. Lett.* **2010**, *97*, 023103. [[CrossRef](#)]
- Sheikhbahai, M.; Esfahany, M.N.; Etesami, N. Experimental investigation of pool boiling of Fe<sub>3</sub>O<sub>4</sub>/ethylene glycol-water nanofluid in electric field. *Int. J. Therm. Sci.* **2012**, *62*, 149–153. [[CrossRef](#)]
- Tang, Y.; Tang, B.; Qing, J.; Li, Q.; Lu, L. Nanoporous metallic surface: Facile fabrication and enhancement of boiling heat transfer. *Appl. Surf. Sci.* **2012**, *258*, 8747–8751. [[CrossRef](#)]
- Betz, A.R.; Jenkins, J.; Attinger, D. Boiling heat transfer on superhydrophilic, superhydrophobic, and superbiphilic surfaces. *Int. J. Heat Mass Transf.* **2013**, *57*, 733–741. [[CrossRef](#)]
- Dai, X.; Huang, X.; Yang, F.; Li, X.; Sightler, J.; Yang, Y.; Li, C. Enhanced nucleate boiling on horizontal hydrophobic-hydrophilic carbon nanotube coatings. *Appl. Phys. Lett.* **2013**, *102*, 161605. [[CrossRef](#)]

28. Kim, J.H.; Gurung, A.; Amaya, M.; Kwark, S.M.; You, S.M. Microporous Coatings to Maximize Pool Boiling Heat Transfer of Saturated R-123 and Water. *J. Heat Transf.* **2015**, *137*, 081501. [[CrossRef](#)]
29. Bostanci, H.; Joshua, N.E. Nucleate Boiling of Dielectric Liquids on Hydrophobic and Hydrophilic Surfaces. In Proceedings of the ASME International Mechanical Engineering Congress and Exposition, Houston, TX, USA, 13–19 November 2015; American Society of Mechanical Engineers: New York, NY, USA, 2015; Volume 57496, p. V08AT10A036.
30. Jun, S.; Wi, H.; Gurung, A.; Amaya, M.; You, S.M. Pool Boiling Heat Transfer Enhancement of Water Using Brazed Copper Microporous Coatings. *J. Heat Transf.* **2016**, *138*, 071502. [[CrossRef](#)]
31. Gao, J.; Lu, L.-S.; Sun, J.-W.; Liu, X.-K.; Tang, B. Enhanced boiling performance of a nanoporous copper surface by electrodeposition and heat treatment. *Heat Mass Transf.* **2016**, *53*, 947–958. [[CrossRef](#)]
32. Hu, H.; Xu, C.; Zhao, Y.; Ziegler, K.J.; Chung, J.N. Boiling and quenching heat transfer advancement by nanoscale surface modification. *Sci. Rep.* **2017**, *7*, 6177. [[CrossRef](#)] [[PubMed](#)]
33. Kumar, U.; Suresh, S.; Thansekhar, M.R.; Babu, D. Effect of diameter of metal nanowires on pool boiling heat transfer with FC-72. *Appl. Surf. Sci.* **2017**, *423*, 509–520. [[CrossRef](#)]
34. Seo, G.H.; Jeong, U.; Son, H.H.; Shin, D.; Kim, S.J. Effects of layer-by-layer assembled PEI/MWCNT surfaces on enhanced pool boiling critical heat flux. *Int. J. Heat Mass Transf.* **2017**, *109*, 564–576. [[CrossRef](#)]
35. Gu, Y.; Xu, S.; Wu, X. Thermal conductivity enhancements and viscosity properties of water based Nanofluid containing carbon nanotubes decorated with ag nanoparticles. *Heat Mass Transf.* **2018**, *54*, 1847–1852. [[CrossRef](#)]
36. Abdel-Rahman, A.A.; Al-Fahed, S.F.; Chakroun, W. The near-field characteristics of circular jets at low Reynolds numbers. *Mech. Res. Commun.* **1996**, *23*, 313–324. [[CrossRef](#)]
37. Freund, L.B.; Suresh, S. *Thin Film Materials: Stress, Defect Formation and Surface Evolution*; Cambridge University Press: Cambridge, UK, 2004.
38. Promvong, P.; Eiamsa-Ard, S. Heat transfer behaviors in a tube with combined conical-ring and twisted-tape insert. *Int. Commun. Heat Mass Transf.* **2007**, *34*, 849–859. [[CrossRef](#)]
39. Nanan, K.; Thianpong, C.; Promvong, P.; Eiamsa-Ard, S. Investigation of heat transfer enhancement by perforated helical twisted-tapes. *Int. Commun. Heat Mass Transf.* **2014**, *52*, 106–112. [[CrossRef](#)]
40. Thianpong, C.; Eiamsa-Ard, P.; Promvong, P.; Eiamsa-Ard, S. Effect of perforated twisted-tapes with parallel wings on heat transfer enhancement in a heat exchanger tube. *Energy Procedia* **2012**, *14*, 1117–1123. [[CrossRef](#)]
41. Thianpong, C.; Yongsiri, K.; Nanan, K.; Eiamsa-Ard, S. Thermal performance evaluation of heat exchangers fitted with twisted-ring turbulators. *Int. Commun. Heat Mass Transf.* **2012**, *39*, 861–868. [[CrossRef](#)]
42. Wongcharee, K.; Eiamsa-Ard, S. Friction and heat transfer characteristics of laminar swirl flow through the round tubes inserted with alternate clockwise and counter-clockwise twisted-tapes. *Int. Commun. Heat Mass Transf.* **2011**, *38*, 348–352. [[CrossRef](#)]
43. Eiamsa-Ard, S.; Promvong, P. Thermal characteristics in round tube fitted with serrated twisted tape. *Appl. Therm. Eng.* **2010**, *30*, 1673–1682. [[CrossRef](#)]
44. Eiamsa-ard, S.; Wongcharee, K.; Eiamsa-Ard, P.; Thianpong, C. Heat transfer enhancement in a tube using del-ta-winglet twisted tape inserts. *Appl. Therm. Eng.* **2010**, *30*, 310–318. [[CrossRef](#)]
45. Eiamsa-Ard, S.; Wongcharee, K.; Sripattanapipat, S. 3-D Numerical simulation of swirling flow and convective heat transfer in a circular tube induced by means of loose-fit twisted tapes. *Int. Commun. Heat Mass Transf.* **2009**, *36*, 947–955. [[CrossRef](#)]
46. Promvong, P.; Pethkool, S.; Pimsarn, M.; Thianpong, C. Heat transfer augmentation in a helical-ribbed tube with double twisted tape inserts. *Int. Commun. Heat Mass Transf.* **2012**, *39*, 953–959. [[CrossRef](#)]
47. Skullong, S.; Promvong, P.; Thianpong, C.; Pimsarn, M. Heat transfer and turbulent flow friction in a round tube with staggered-winglet perforated-tapes. *Int. J. Heat Mass Transf.* **2016**, *95*, 230–242. [[CrossRef](#)]
48. Pethkool, S.; Eiamsa-Ard, S.; Kwankaomeng, S.; Promvong, P. Turbulent heat transfer enhancement in a heat exchanger using helically corrugated tube. *Int. Commun. Heat Mass Transf.* **2010**, *38*, 340–347. [[CrossRef](#)]
49. Kongkaitpaiboon, V.; Nanan, K.; Eiamsa-Ard, S. Experimental investigation of heat transfer and turbulent flow friction in a tube fitted with perforated conical-rings. *Int. Commun. Heat Mass Transf.* **2010**, *37*, 560–567. [[CrossRef](#)]
50. Guo, J.; Fan, A.; Zhang, X.; Liu, W. A numerical study on heat transfer and friction factor characteristics of laminar flow in a circular tube fitted with center-cleared twisted tape. *Int. J. Therm. Sci.* **2011**, *50*, 1263–1270. [[CrossRef](#)]
51. Chang, S.W.; Jan, Y.J.; Liou, J.S. Turbulent heat transfer and pressure drop in tube fitted with serrated twisted tape. *Int. J. Therm. Sci.* **2007**, *46*, 506–518. [[CrossRef](#)]
52. Kathait, P.S.; Patil, A.K. Thermo-hydraulic performance of a heat exchanger tube with discrete corrugations. *Appl. Therm. Eng.* **2014**, *66*, 162–170. [[CrossRef](#)]
53. Vashistha, C.; Patil, A.K.; Kumar, M. Experimental investigation of heat transfer and pressure drop in a circular tube with multiple inserts. *Appl. Therm. Eng.* **2016**, *96*, 117–129. [[CrossRef](#)]
54. Li, H.M.; Ye, K.S.; Tan, Y.; Deng, S.J. Investigation on tube-side flow visualization, friction factors and heat transfer characteristics of helical-ridging tubes. In Proceedings of the International Heat Transfer Conference Digital Library, Munich, Germany, 6–10 September 1982; Begel House Inc.: Danbury, CT, USA, 1982.
55. Wen, D.; Ding, Y. Experimental investigation into convective heat transfer of nanofluid at the entrance region under laminar flow conditions. *Int. J. Heat. Mass. Transf.* **2004**, *47*, 5181–5188. [[CrossRef](#)]

56. Kim, S.J.; Bang, I.C.; Buongiorno, J.; Hu, L.W. Surface wettability change during pool boiling of nanofluids and its effect on critical heat flux. *Int. J. Heat Mass Transf.* **2007**, *50*, 4105–4116. [[CrossRef](#)]
57. Amirahmad, A.; Maglad, A.M.; Mustafa, J.; Cheraghian, G. Loading PCM Into Buildings Envelope to Decrease Heat Gain-Performing Transient Thermal Analysis on Nanofluid Filled Solar System. *Front. Energy Res.* **2021**, *9*, 727011. [[CrossRef](#)]
58. Gunnasegaran, P.; Shuaib, N.H.; Jalal, M.F.A.; Sandhita, E. Numerical Study of Fluid Dynamic and Heat Transfer in a Compact Heat Exchanger Using Nanofluids. *Int. Sch. Res. Not.* **2012**, *2012*, 585496. [[CrossRef](#)]
59. Maddah, H.; Alizadeh, M.; Ghasemi, N.; Alwi, S.R.W. Experimental study of Al<sub>2</sub>O<sub>3</sub>/water nanofluid turbulent heat transfer enhancement in the horizontal double pipes fitted with modified twisted tapes. *Int. J. Heat Mass Transf.* **2014**, *78*, 1042–1054. [[CrossRef](#)]
60. Maddah, H.; Aghayari, R.; Mirzaee, M.; Ahmadi, M.H.; Sadeghzadeh, M.; Chamkha, A.J. Factorial experimental design for the thermal performance of a double pipe heat exchanger using Al<sub>2</sub>O<sub>3</sub>-TiO<sub>2</sub> hybrid nanofluid. *Int. Commun. Heat Mass Transf.* **2018**, *97*, 92–102. [[CrossRef](#)]
61. Freitas, E.; Pontes, P.; Cautela, R.; Bahadur, V.; Miranda, J.; Ribeiro, A.P.C.; Souza, R.R.; Oliveira, J.D.; Copetti, J.B.; Lima, R.; et al. Pool Boiling of Nanofluids on Biphilic Surfaces: An Experimental and Numerical Study. *Nanomaterials* **2021**, *11*, 125. [[CrossRef](#)]
62. Pasandideh-Fard, M.; Chandra, S.; Mostaghimi, J. A three-dimensional model of droplet impact and solidification. *Int. J. Heat Mass Transf.* **2002**, *45*, 2229–2242. [[CrossRef](#)]
63. Larsen, T.S.; Nikolopoulos, N.; Nikolopoulos, A.; Strotos, G.; Nikas, K.-S. Characterization and prediction of the volume flow rate aerating a cross ventilated building by means of experimental techniques and numerical approaches. *Energy Build.* **2011**, *43*, 1371–1381. [[CrossRef](#)]
64. Roisman, I.V. Inertia dominated drop collisions. II. An analytical solution of the Navier–Stokes equations for a spreading viscous film. *Phys. Fluids* **2009**, *21*, 052104. [[CrossRef](#)]
65. Herbert, S.; Gambaryan-Roisman, T.; Stephan, P. Influence of the governing dimensionless parameters on heat transfer during single drop impingement onto a hot wall. *Colloids Surf. A Physicochem. Eng. Asp.* **2013**, *432*, 57–63. [[CrossRef](#)]
66. Ahn, H.S.; Kim, J.; Kim, M.H. Investigation of Pool Boiling Critical Heat Flux Enhancement on a Modified Surface Through the Dynamic Wetting of Water Droplets. *J. Heat Transf.* **2012**, *134*, 071504. [[CrossRef](#)]
67. Alizadeh, A.; Bahadur, V.; Zhong, S.; Shang, W.; Li, R.; Ruud, J.A.; Yamada, M.; Ge, L.; Dhinojwala, A.; Sohal, M. Temperature dependent droplet impact dynamics on flat and textured surfaces. *Appl. Phys. Lett.* **2012**, *100*, 111601. [[CrossRef](#)]
68. Negeed, E.-S.R.; Albeirutty, M.; Takata, Y. Dynamic behavior of micrometric single water droplets impacting onto heated surfaces with TiO<sub>2</sub> hydrophilic coating. *Int. J. Therm. Sci.* **2014**, *79*, 1–17. [[CrossRef](#)]
69. Tran, T.; Staat, H.J.J.; Prosperetti, A.; Sun, C.; Lohse, D. Drop Impact on Superheated Surfaces. *Phys. Rev. Lett.* **2012**, *108*, 036101. [[CrossRef](#)] [[PubMed](#)]
70. Moon, J.H.; Cho, M.; Lee, S.H. Dynamic wetting and heat transfer characteristics of a liquid droplet impinging on heated textured surfaces. *Int. J. Heat Mass Transf.* **2016**, *97*, 308–317. [[CrossRef](#)]
71. Zuber, N. On the stability of boiling heat transfer. *Trans. Am. Soc. Mech. Eng.* **1958**, *80*, 711–714. [[CrossRef](#)]
72. Mikic, B.B.; Rohsenow, W.M. A new correlation of pool-boiling data including the effect of heating surface characteristics. *J. Heat Transf.* **1969**, *91*, 245–250. [[CrossRef](#)]
73. Prasad, N.R.; Saini, J.S.; Prakash, R. The effect of heater wall thickness on heat transfer in nucleate pool-boiling at high heat flux. *Int. J. Heat Mass Transf.* **1985**, *28*, 1367–1375. [[CrossRef](#)]
74. Bhat, A.M.; Prakash, R.T.; Saini, J.S. On the mechanism of macrolayer formation in nucleate pool boiling at high heat flux. *Int. J. Heat Mass Transf.* **1983**, *26*, 735–740. [[CrossRef](#)]
75. Jairajpuri, A.M.; Saini, J.S. A new model for heat flow through macrolayer in pool boiling at high heat flux. *Int. J. Heat Mass Transf.* **1991**, *34*, 1579–1591. [[CrossRef](#)]
76. Pasamehmetoglu, K.O.; Chappidi, P.R.; Unal, C.; Nelson, R.A. Saturated pool nucleate boiling mechanisms at high heat fluxes. *Int. J. Heat Mass Transf.* **1993**, *36*, 3859–3868. [[CrossRef](#)]
77. Katto, Y. Critical heat flux. *Int. J. Multiph. Flow* **1994**, *20*, 53–90. [[CrossRef](#)]
78. Lienhard, J.H. Snares of pool boiling research: Putting our history to use. *Heat Transf.* **1994**, *1*, 333–348.
79. Das, S.K.; Roetzel, W. A Composite Heat Transfer Model For Pool Boiling on a Horizontal Tube at Moderate Pressure. *Can. J. Chem. Eng.* **2008**, *82*, 316–322. [[CrossRef](#)]
80. Sateesh, G.; Das, S.K.; Balakrishnan, A.R. Analysis of pool boiling heat transfer: Effect of bubbles sliding on the heating surface. *Int. J. Heat Mass Transf.* **2005**, *48*, 1543–1553. [[CrossRef](#)]
81. Qu, X.; Revankar, S.T.; Tian, M. Numerical simulation of bubble formation and condensation of steam air mixture injected in subcooled pool. *Nucl. Eng. Des.* **2017**, *320*, 123–132. [[CrossRef](#)]
82. Ribatski, G.; Jabardo, J.M. Experimental study of nucleate boiling of halocarbon refrigerants on cylindrical surfaces. *Int. J. Heat Mass Transf.* **2003**, *46*, 4439–4451. [[CrossRef](#)]
83. Elghanam, R.I.; Fawal, M.E.; Aziz, R.A.; Skr, M.; Khalifa, A.H. Experimental study of nucleate boiling heat transfer enhancement by using surfactant. *Ain Shams Eng. J.* **2011**, *2*, 195–209. [[CrossRef](#)]
84. Das, A.K.; Das, P.K.; Saha, P. Performance of different structured surfaces in nucleate pool boiling. *Appl. Therm. Eng.* **2009**, *29*, 3643–3653. [[CrossRef](#)]

85. Mehta, J.S.; Kandlikar, S.G. Pool boiling heat transfer enhancement over cylindrical tubes with water at atmospheric pressure, Part I: Experimental results for circumferential rectangular open microchannels. *Int. J. Heat Mass Transf.* **2013**, *64*, 1205–1215. [[CrossRef](#)]
86. Meena, C.S.; Deep, A.; Das, A.K. Understanding of Interactions for Bubbles Generated at Neighboring Nucleation Sites. *Heat Transf. Eng.* **2017**, *39*, 885–900. [[CrossRef](#)]
87. Deep, A.; Meena, C.S.; Das, A.K. Interaction of Asymmetric Films Around Boiling Cylinder Array: Homogeneous Interface to Chaotic Phenomenon. *J. Heat Transf.* **2017**, *139*, 041502. [[CrossRef](#)]
88. Yamagata, K.; Hirano, F.; Nishikawa, K.; Matsuoka, H. Nucleate boiling of water on the horizontal heating surface. *Mem. Fac. Eng. Kyushu* **1955**, *15*, 98.
89. Kurihara, H.M.; Myers, J.E. The effects of superheat and surface roughness on boiling coefficients. *AIChE J.* **1960**, *6*, 83–91. [[CrossRef](#)]
90. Hsu, S.T.; Schmidt, F.W. Measured Variations in Local Surface Temperatures in Pool Boiling of Water. *J. Heat Transf.* **1961**, *83*, 254–260. [[CrossRef](#)]
91. Hsu, Y.Y. On the Size Range of Active Nucleation Cavities on a Heating Surface. *J. Heat Transf.* **1962**, *84*, 207–213. [[CrossRef](#)]
92. Hsu, Y.Y.; Graham, R.W. *Transport Processes in Boiling and Two-Phase Systems, including Near-Critical Fluids*; Hemisphere Publishing Corp.: Washington, DC, USA; McGraw-Hill Book Co.: New York, NY, USA, 1976; p. 559.
93. Gaertner, R.F.; Westwater, J.W. *Population of Active Sites in Nucleate Boiling Heat Transfer*; ProQuest Dissertations Publishing: Ann Arbor, MI, USA, 1960; Volume 56.
94. Cornwell, K.; Brown, R.D. Boiling Surface topography. In Proceedings of the 6th International Heat Transfer Conference, Toronto, ON, Canada, 7–11 August 1978; Volume 1, pp. 157–161.
95. Rohsenow, W.M. *A Method of Correlating Heat-Transfer Data for Surface Boiling of Liquids*; MIT Division of Industrial Cooperation: Cambridge, MA, USA, 1952.